Multiscale modeling approach for
thermal buckling analysis of nanocomposite curved structure

Kulmani Mehar [1a] and Subrata Kumar Panda[*2]

[1] *Department of Mechanical Engineering, Madanapalle Institute of Technology & Science, Madanapalle, India*
[2] *Department of Mechanical Engineering, National Institute of Technology Rourkela, Odisha, 769008, India*

Abstract. The thermal buckling temperature values of the graded carbon nanotube reinforced composite shell structure is explored using higher-order mid-plane kinematics and multiscale constituent modeling under two different thermal fields. The critical values of buckling temperature including the effect of in-plane thermal loading are computed numerically by minimizing the final energy expression through a linear isoparametric finite element technique. The governing equation of the multiscale nanocomposite is derived via the variational principle including the geometrical distortion through Green-Lagrange strain. Additionally, the model includes different grading patterns of nanotube through the panel thickness to improve the structural strength. The reliability and accuracy of the developed finite element model are varified by comparison and convergence studies. Finally, the applicability of present developed model was highlight by enlighten several numerical examples for various type shell geometries and design parameters.

Keywords: thermal buckling; FG-CNT; HSDT; thermal load; FEM; micromechanical model

1. Introduction

Thermal buckling is the geometrical instability induced in the structural member due to the in-plane loading and the structural configuration may deviate from the equilibrium path. However, the initiation of buckling does not indicate the final failure of that structure and it can withstand extra amount of load even after the excess deformation. To examine the thermal buckling responses the laminated and functionally graded composite structure, a number of research articles have been published (Szekrenyes 2014, Moradi-Dastjerdi *et al.* 2017, Han *et al.* 2017, Rafiee *et al.* 2018). Zenkour (2005) implemented the various types of displacement dependent shear deformation theories to compute the buckling load parameter of the functionally grated material (FGM) composite sandwich plate. Similarly, the mechanical buckling responses of the cracked thin composite plate is analyzed under the tensile and compressive loading (Brighenti 2005a, b). Further, the boundary element method is adopted to explore the buckling load parameters of composite structure under the in-plane mechanical loading (Baiz and Aliabadi 2007). The thermal post-buckling characteristic of the isotropic material (steel) and laminated composite (graphite/epoxy composite) plates based on the higher-order shear deformation theory (HSDT) were computed and validated with the experimental result (Amabili and Tajahmadi 2012, Reddy *et al.* 2013, Bouadi *et al.* 2018, Torabi *et al.* 2019).

The thermomechanical post-buckling response of the FGM composite plate was computed by employing the HSDT and von-Karman geometrical nonlinearity (Rafiee *et al.* 2013; Bakora and Tounsi 2015). An extensive literature review of the bending, vibration and buckling behaviors of the FGM composite was performed in 2015 (Swaminathan *et al.* 2015).

Further, the first time in 2009, the functionally graded concept has been implemented to illustrate the mechanical static behavior of the graded carbon nanotube reinforced composite (CNTRC) (Shen 2009). The thermal buckling and post-buckling responses of the functionally graded carbon nanotube reinforced composite (FG-CNTRC) were estimated using Reddy's HSDT kinematic model (Shen and Zhang 2010), in which one uniformly distributed carbon nanotube (CNT) and three functionally graded CNT distribution patterns were used and the effective material properties of the composite were estimated by a micromechanics model. Using the similar micromechanics model, the mechanical buckling and post-buckling responses of the FG-CNTRC were estimated under uniaxial tensile mechanical load under thermal environment (Shen and Zhu 2010). Later, this work was extended for the cylindrical shell geometry and computed the mechanical bucking load of the FG-CNTRC cylindrical panel by employed the higher-order polynomial equation (Shen 2011). The thermal buckling was also calculated for the cylindrical shell panel (Shen 2012, Nejati *et al.* 2017). From the numerical results, it is found that the thermal and mechanical buckling, as well as post-buckling responses, improve with the higher CNT volume fraction. In addition to the above, the nonlocal Timoshenko beam model used to examine the buckling behavior of CNT (Zidour *et al.* 2014).

*Corresponding author, Associate Profesor,
E-mail: call2subrat@gmail.com; pandask@nitrkl.ac.in
[a] Assistant Professor, E-mail: kulmanimehar@gmail.com

Also, Timoshenko beam theory was employed to estimate the vibration behavior of the CNT. The mechanical buckling performance of the FG-CNTRC plate was computed using the FSDT kinematics by assumed that the single walled carbon nanotubes were aligned along the length or randomly oriented (Mehrabadi *et al*. 2012, Farzam and Hassani 2018). In which, the effective properties of the composite material were investigated by Mori-Tanaka method or the rule of mixture. The buckling responses of the CNT reinforced annular and circular section composite based on the HSDT kinematics were computed using the finite element method (FEM) (Maghamikia and Jam 2011).

The dynamic buckling behavior of the CNTRC beam under three combined loads (thermal, electrical and mechanical) was computed by Yang *et al*. (2015). Zhang *et al*. (2015a) analyzed the buckling behavior of the graded composite plate reinforced with the single-walled carbon nanotube (SW-CNT) and resting on the elastic foundation by employing the element-free IMLS-Ritz method. Also, the element free method was implemented to demonstrate the buckling behavior of the FG-CNTRC skew plate (Lei *et al*. 2015, Zhang *et al*. 2015b). Further, the bending, buckling and vibration behavior of the graded CNT reinforced beam were estimated with non-uniform temperature load (Mayandi and Jeyaraj 2015). The mechanical buckling behavior of the CNTRC conical shell panel was highlighted under uniaxial compressive load (Ansari and Torabi 2016) by implementing Hamiton's principle and generalized differential quadrature method. Further, buckling and vibration characteristics of the annular composite plate reinforced with the CNT were computed under thermal load (Ansari *et al*. 2017). The first-order shear deformation theory (FSDT) kinematics used to figure out the buckling and post-buckling critical temperature of the CNT reinforced composite plate (Mirzaei and Kiani 2016). Additionally, FSDT kinematics implemented to computed the mechanical buckling of the nanotube-reinforced graded composite plate under parabolic loading condition (Kiani 2017). The mechanical and thermal buckling load parameter of the truncated conical structure reinforced with graded CNT were computed by employing Galerkin method (Duc *et al*. 2017). The influence of the CNT agglomeration on the buckling and frequency load parameters of the composite plate reinforced via CNT were computed by considering the nonlocal effect based on the Eringen's nonlocal theory (Kolahchi and Cheraghbak 2017). Kolahchi (2017) implemented the nonlocal theories to demonstrate the vibration, flexural and buckling characteristics of the nano-plate. Additionally, many other research works have been presented to highlight the bending, vibration and buckling characteristics of the different type composite structure such as laminated, FGM and FG-. Today, composite structure analysis is divided in mainly two ways, first improve the mathematical model or analysis technique to obtain the realistic responses with minimum time of computation and secondly improve the desired responses by introducing new material or modification of the structure. Tounsi and co-authors have done remarkable work to reduce the number of variables of the shear deformation theories and computed the vibration,

bending and buckling responses of different type composite structures (Berrabah *et al*. 2013, Draiche *et al*. 2014, Hamidi *et al*. 2015).

The extensive review reveals that sufficient research works have been establish the bending, buckling and vibration behavior of the CNTRC structure using different available shear deformation theories. However, most of the works are based on the FSDT and only few works have been presented for the buckling analysis of the FG-CNTRC. Based on the authors' knowledge buckling behavior of the FG-CNTRC based on the HSDT kinematics in conjunction with FEM is not available in open literature. To fulfil such gap, thermal instability of the FG-CNTRC shell panel based on the HSDT mid-plane kinematics has been evaluated via FEM and highlighted the effect of various design parameter on the thermal instability of composite shell panel reinforced with single-walled carbon nanotube (SWCNT). It is assumed that the material properties are graded along transverse direction and evaluated using the extended rule of mixture. The final form of governing equilibrium equation solved computationally via the home-made FE code in MATLAB environment. The reliability and accuracy of the computed buckling temperature data verified through proper comparison study including the convergence test. Finally, the applicability of the derived multiscale numerical model is highlighted by solving variable numerical examples and deliberated with simultaneous reasons.

2. Theory and formulations

buckling temperature under thermal environment. Fig. 1 depicted the geometry of the FG-CNTRC shell panel with curvature R_1 and R_2 about X and Y-axis, respectively. In composite structure analysis, number of research works are going on to increase the critical buckling temperature of the composite structure and it can be attained by improving the geometrical configuration and material distribution patterns. In the present study, four different CNT grading patterns and four type shell geometries are used to obtain the thermal stability of the FG-CNTRC shell panel. The geometry of the curved shell panel can be defined with respect to curvature such as cylindrical (CYL - in which one radius is R and other is infinite), spherical (SPH – both
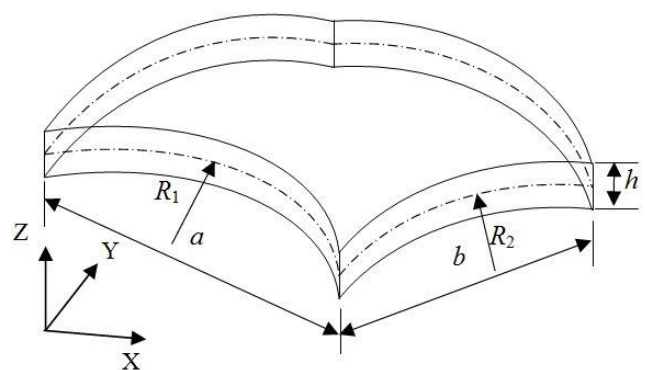

Fig. 1 Geometry of curved shell panel

curvatures are equal to R), elliptical (ELL - one curvature is double of the other curvature, $R_x = 0.5R_y = R$) and hyperbolic (HYP - both curvatures are opposite sign, $R_x = -R_y = R$). CNT distributions is used in four different types such as: UD (CNTs are uniformally distributed in *XY*-plane), FG-X (CNTs are maximum at the top and bottom surface and zero at the middle of of composit panel), FG-O (CNTs are maximum at the mid-plane and gradually decreses toward the top and bottom surfaces) and FG-V (CNTs maximum at the top surface and gradually decreases toward the bottom surface). The mathematical expression for the CNT distribution can better understand from mathematical expression as follows

$$V_{NT}(z) = \begin{cases} V_{NT}^* & (UD) \\ 2\left(1 - \dfrac{2|z|}{h}\right)V_{NT}^* & (FG-O) \\ \left(1 + \dfrac{2z}{h}\right)V_{NT}^* & (FG-V) \\ 2\left(\dfrac{2|z|}{h}\right)V_{NT}^* & (FG-X) \end{cases} \quad (1)$$

V_{NT}^* represents the total CNT volume fraction within the composite, however V_{NT} represents the graded CNT volume fraction varying in *Z*-direction.

Due to the grading of the CNT volume fraction in *Z*-direction, other material properties also graded according to the CNT volume fraction. To evaluate the graded material properties of the composite, the rule of mixture was implemented with effectiveness parameters of the CNT, such as

$$E_{1C} = \eta_1 V_{NT} E_{1NT} + V_m E_m \quad (2)$$

$$\frac{\eta_2}{E_{2C}} = \frac{V_{NT}}{E_{2NT}} + \frac{V_m}{E_m} \quad (3)$$

$$\frac{\eta_3}{G_{12C}} = \frac{V_{NT}}{G_{12NT}} + \frac{V_m}{G_m} \quad (4)$$

where, E_{11} and E_{22} are the elastic modulus along the fiber, and normal of fibers, respectively. G_{12} represents for the modulus of rigidity and "*V*" represents for the volume fraction. The subscript "*NT*", "*m*" and '*C*' represents for the nanotube, matrix and CNT/matrix composite, respectively. Additionally, η_1, η_2 and η_3 are the effectiveness parameters for the CNT within the composite and these are obtained by comparing the results of molecular dynamic simulation results and the rule of mixture results (Shen 2012).

Similarly, the other material properties density (ρ_C), Poisson's ratio (υ_{12C}) and coefficients of thermal expansion (α_{1C} and α_{2C}) are computed using the formulae explained in reference

$$\upsilon_{12C} = V_{NT}\upsilon_{12NT} + V_m\upsilon_m \quad (5)$$

$$\rho_C = V_{NT}\rho_{NT} + V_m\rho_m \quad (6)$$

$$\alpha_{1C} = \frac{\alpha_{1NT}V_{NT}E_{1NT} + \alpha_m V_m E_m}{V_{NT}E_{1NT} + V_m E_m} \quad (7)$$

$$\alpha_{2C} = (1 + \upsilon_{12NT})V_{NT}\alpha_{2NT} + (1 + \upsilon_m)V_m\alpha_m - \upsilon_{12C}\alpha_{1C} \quad (8)$$

In present analysis, it is assumed that the material properties of the each element (CNT and polymer) are the function of temperature. Also, assumed that the temperature is graded in the normal direction of shell panel with two different type temperature distributions namely, uniformly distributed temperature (UDT) and linearly distributed temperature (LDT). In the UDT profile temperature is assumed to be constant over the entered composite plate. However, in the case of the LDT, the temperature profile is assumed to linearly increase from the bottom surface (room temperature, $T_0 = 300$ K) to the top surface of the composite (Fazzolari 2015).

$$T(z) = T_0 + (T_3 - T_0)\left(\frac{z}{h} + \frac{1}{2}\right) \quad (9)$$

The numerical model of the SWCNT/polymer composite shell structure is formulated via the HSDT mid-plane kinematics. The global displacement component (u_x, u_y and u_z) of a point in the composite shell panel are function of 9-unknown parameters (u_{x0}, u_{y0}, u_{z0}, φ_x, φ_y, ψ_x, ψ_y, θ_x and θ_y,) (Pandya and Kant 1988). The displacement field of the composite shell panel is obtained using Taylor's series and defined as

$$\begin{aligned} u_x &= u_{x0} + z\varphi_x + z^2\psi_x + z^3\theta_x \\ u_y &= u_{y0} + z\varphi_y + z^2\psi_y + z^3\theta_y \\ u_z &= u_{z0} \end{aligned} \quad (10)$$

where, u_{x0}, u_{y0} and u_{z0} are the midplane displacements component of any point in three mutual perpendicular directions along the *X*, *Y* and *Z*-directions, respectively. φ_x and φ_y are midplane rotational terms and (ψ_x, ψ_y, θ_x and θ_y) are higher order terms. These unknown parameters are defined as $u_{x0} = u_x$, $u_{y0} = u_y$, $u_{z0} = u_z$, $\varphi_x = \frac{\partial u_x}{\partial z}$, $\varphi_y = \frac{\partial u_y}{\partial z}$, $\psi_x = \frac{1}{2}\left(\frac{\partial^2 u_x}{\partial z^2}\right)$, $\psi_y = \frac{1}{2}\left(\frac{\partial^2 u_y}{\partial z^2}\right)$, $\theta_x = \frac{1}{6}\left(\frac{\partial^3 u_x}{\partial z^3}\right)$ and $\theta_y = \frac{1}{6}\left(\frac{\partial^3 u_y}{\partial z^3}\right)$, when $z = 0$.

The Eq. (10) can be rewritten in the matrix form as

$$\{\lambda\} = [H_1]\{\lambda_0\} \quad (11)$$

where, $\{\lambda\} = \{u_x \ u_y \ u_z\}^T$ is the represent for the displacement of any point within the composite, $\{\lambda_0\} = \{u_{x0} \ u_{y0} \ u_{z0} \ \varphi_x \ \varphi_y \ \psi_x \ \psi_y \ \theta_x \ \theta_y\}^T$ is the vector of displacement at $z = 0$ and $[H_1]$ is known as thickness co-ordinate matrix

$$[H_1] = \begin{bmatrix} 1 & 0 & 0 & z & 0 & z^2 & 0 & z^3 & 0 \\ 0 & 1 & 0 & 0 & z & 0 & z^2 & 0 & z^3 \\ 0 & 0 & 1 & 0 & 0 & 0 & 0 & 0 & 0 \end{bmatrix} \quad (12)$$

The strain-displacement field of polymer composite structure reinforced with CNT is

$$\{\varepsilon\} = \begin{Bmatrix} \varepsilon_{xx} \\ \varepsilon_{yy} \\ \gamma_{xy} \\ \gamma_{zx} \\ \gamma_{yz} \end{Bmatrix} = \begin{Bmatrix} \dfrac{\partial u_x}{\partial x} + \dfrac{u_z}{R_x} \\[6pt] \dfrac{\partial u_y}{\partial y} + \dfrac{u_z}{R_y} \\[6pt] \dfrac{\partial u_x}{\partial y} + \dfrac{\partial u_y}{\partial x} + \dfrac{2w}{R_{xy}} \\[6pt] \dfrac{\partial u_x}{\partial z} + \dfrac{\partial u_z}{\partial x} - \dfrac{u_x}{R_x} \\[6pt] \dfrac{\partial u_y}{\partial z} + \dfrac{\partial u_z}{\partial y} - \dfrac{u_y}{R_y} \end{Bmatrix} \quad (13)$$

By substituting the displacement terms u_x, u_y and u_z in above equation.

$$\{\varepsilon\} = \begin{Bmatrix} \varepsilon_x^0 \\ \varepsilon_y^0 \\ \varepsilon_{xy}^0 \\ \varepsilon_{xz}^0 \\ \varepsilon_{yz}^0 \end{Bmatrix} + z\begin{Bmatrix} k_x^1 \\ k_y^1 \\ k_{xy}^1 \\ k_{zx}^1 \\ k_{yz}^1 \end{Bmatrix} + z^2\begin{Bmatrix} k_x^2 \\ k_y^2 \\ k_{xy}^2 \\ k_{zx}^2 \\ k_{yz}^2 \end{Bmatrix} + z^3\begin{Bmatrix} k_x^3 \\ k_y^3 \\ k_{xy}^3 \\ k_{zx}^3 \\ k_{yz}^3 \end{Bmatrix} \quad (14)$$

or $\qquad \{\varepsilon\} = [H_2]\{\bar{\varepsilon}\}$

where, $[H_2]_{5\times 20} = [I_1 \ z\times I_1 \ z^2\times I_1 \ z^3\times I_1]$ is the thickness coordinate matrix and $\{\bar{\varepsilon}\} = \{\varepsilon_x^0 \ \varepsilon_y^0 \ \varepsilon_{xy}^0 \ \varepsilon_{xz}^0 \ \varepsilon_{yz}^0 \ k_x^1 \ k_y^1 \ k_{xy}^1 \ k_{zx}^1 \ k_{yz}^1 \ k_x^2 \ k_y^2 \ k_{xy}^2 \ k_{zx}^2 \ k_{yz}^2 \ k_x^3 \ k_y^3 \ k_{xy}^3 \ k_{zx}^3 \ k_{yz}^3\} = [B]\{\lambda_0\}$. $[I_1]$ is a unit matrix of 5×5.

The thermoelastic constitutive relations of the graded composite structure reinforced with the CNT can be written as

$$\begin{Bmatrix} \sigma_{xx} \\ \sigma_{yy} \\ \tau_{xy} \\ \tau_{zx} \\ \tau_{yz} \end{Bmatrix} = \begin{bmatrix} C_{11} & C_{12} & 0 & 0 & 0 \\ C_{21} & C_{22} & 0 & 0 & 0 \\ 0 & 0 & C_{66} & 0 & 0 \\ 0 & 0 & 0 & C_{44} & 0 \\ 0 & 0 & 0 & 0 & C_{55} \end{bmatrix} \left(\begin{Bmatrix} \varepsilon_{xx} \\ \varepsilon_{yy} \\ \gamma_{xy} \\ \gamma_{zx} \\ \gamma_{yz} \end{Bmatrix} - \begin{Bmatrix} \alpha_{11} \\ \alpha_{22} \\ 0 \\ 0 \\ 0 \end{Bmatrix} \Delta T \right) \quad (15)$$

or $\{\sigma\} = [C_{ij}]\{\varepsilon - \alpha\Delta T\}$

where, $C_{11} = E_{1C}/(1 - v_{12C}v_{21C})$, $C_{12} = v_{12C}E_{2C}/(1 - v_{12C}v_{21C})$, $C_{22} = E_{2C}/(1 - v_{12C}v_{21C})$, $C_{66} = G_{12C}$, $C_{44} = G_{13C}$ and $C_{55} = G_{23C}$. $G_{13} = G_{12}$ and $G_{23C} = 1.2\times G_{12}$ are shear modulus. 'ΔT' represent for the temperature change.

The total strain energy of the composite structure calculated as

$$U = \frac{1}{2}\iint\left(\int_{-h/2}^{h/2} \{\varepsilon\}^T\{\sigma\}dz\right)dxdy$$

or $U = \frac{1}{2}\iint\left(\int_{-h/2}^{h/2} \{\bar{\varepsilon}\}^T[H_2]^T\{C_{ij}\}[H_2]\{\bar{\varepsilon}\}dz\right)dxdy$ (16)

or $U = \frac{1}{2}\iint\left(\int_{-h/2}^{h/2} \{\lambda_0\}^T[B]^T[H_2]^T\{C_{ij}\}[H_2][B]\{\lambda_0\}dz\right)dxdy$ (16)

or $U = \frac{1}{2}\iint\{\lambda_0\}^T[B]^T[D][B]\{\lambda_0\}dxdy$

where, $[D] = \int_{-h/2}^{h/2}[H_2]^T\left[C_{ij}\right][H_2]dz$.

The FG-CNTRC composite plate subjected in-plane thermal load and obtained as

$$\{f_T\} = \{N_{xT} \ N_{yT} \ N_{xyT} \ 0 \ 0\}^T = \int_{-h/2}^{h/2}\left[C_{ij}\right]\{\alpha_{1C} \ \alpha_{2C} \ 0 \ 0 \ 0\}^T \Delta T \ dz \ (17)$$

The in-plane thermal work done of the composite can computed as

$$W_T = \int_V \left(\frac{1}{2}\left\{(u_{x,x})^2 + (u_{y,x})^2 + (u_{z,x})^2\right\}N_{xT} + \frac{1}{2}\left\{(u_{x,y})^2 + (u_{y,y})^2 + (u_{z,y})^2\right\}N_{yT} \atop + \{u_{x,x}u_{x,y} + u_{y,x}u_{y,y} + u_{z,x}u_{z,y}\}N_{xyT} \right)dV$$

or $$W_T = \int_V \begin{Bmatrix} u_{x,x} \\ u_{x,y} \\ u_{y,x} \\ u_{y,y} \\ u_{z,x} \\ u_{z,y} \end{Bmatrix}^T \begin{bmatrix} N_{xT} & N_{xyT} & 0 & 0 & 0 & 0 \\ N_{xyT} & N_{yT} & 0 & 0 & 0 & 0 \\ 0 & 0 & N_{xT} & N_{xyT} & 0 & 0 \\ 0 & 0 & N_{xyT} & N_{yT} & 0 & 0 \\ 0 & 0 & 0 & 0 & N_{xT} & N_{xyT} \\ 0 & 0 & 0 & 0 & N_{xyT} & N_{yT} \end{bmatrix} \begin{Bmatrix} u_{x,x} \\ u_{x,y} \\ u_{y,x} \\ u_{y,y} \\ u_{z,x} \\ u_{z,y} \end{Bmatrix} dV \quad (18)$$

or $W_T = \int_V \{\varepsilon_G\}^T[S_T]\{\varepsilon_G\}dV$

or $W_T = \int_V \{\bar{\varepsilon}_G\}^T[H_G]^T[S_T][H_G]\{\bar{\varepsilon}_G\}dV$

or $W_T = \iint\{\bar{\varepsilon}_G\}^T[D_G]\{\bar{\varepsilon}_G\}dxdy$

where, $\{\bar{\varepsilon}_G\} = \{u_{x,x} \ u_{x,y} \ u_{y,x} \ u_{y,x} \ u_{z,x} \ u_{z,y}\}^T$ is the geometric strain terms at mid-plane and $[H_G]_{6\times 24} = [I_1 \ z\times I_1 \ z^2\times I_1 \ z^3\times I_1]$ is a thickness co-ordinate matrix, respectively. $[I]$. $[D_G] = \int_{-h/2}^{h/2}[H_G]^T[S_T][H_G]dz$ denoting a 24×24 material property matrix.

From last few decades, uses of FEM for structural analysis have been increased because it is suitable to solve complicated problem. Now, FEM has been used to find the buckling response of the FG-CNTRC. In which, an isoparametric element of 9-noded with 9-degrees of freedom at each node is employed to divide the composite panel in a number of the element.

The displacement vector at $\{\lambda_0\}$ mid-plane of composite in terms of shape function can be written as follows (Cook *et al.* 2009)

$$\{\lambda_0\} = \sum_{i=1}^{9} N_i\{\lambda_{0i}\} \quad (19)$$

where, N_i is the interpolation function corresponding of 'i^{th}' node and $\{\lambda_{0i}\} = [u_{x0_i} \ u_{y0_i} \ u_{z0_i} \ \varphi_{x_i} \ \varphi_{y_i} \ \psi_{x_i} \ \psi_{y_i} \ \theta_{x_i} \ \theta_{y_i}]^T$ is the displacement vector of 'i^{th}' node.

$\{\bar{\varepsilon}_L\}$ and $\{\bar{\varepsilon}_G\}$ are the strain vectors at $z = 0$ can be written in the form of $\{\lambda_{0i}\}$

$$\{\overline{\varepsilon}_L\} = [B]\{\lambda_{0i}\} \quad (20)$$

$$\{\overline{\varepsilon}_G\} = [B_G]\{\lambda_{0i}\} \quad (21)$$

where, $[B]$ and $[B_G]$ are contained the interpolation function and differential operators.

The variational principle has been espoused to find the equilibrium governing equation for buckling analysis and written as

$$\delta\Pi = \delta(U - W_T) = 0 \quad (22)$$

By rearranging the equilibrium governing Eq. (22), it can be written in the form of eigen-value and eigen-vector as

$$\left(([K_L]) + \gamma_{cr}[K_G]\right)\{\Delta\} = 0 \quad (23)$$

where, γ_{cr} represent for the load factor of critical buckling.

Support conditions used for numerical analysis are:

(a) For simply supported conditions (S):

$u_x = u_z = \varphi_x = \theta_x = \psi_x = 0$ at $y = 0, b$ and
$u_y = u_z = \varphi_y = \theta_y = \psi_y = 0$ at $x = 0, a$

(b) For clamped conditions (C):

$u_x = u_y = u_z = \varphi_x = \varphi_y = \theta_x = \theta_y = \psi_x = \psi_y = 0$
for $y = 0, b$ and $x = 0, a$.

3. Results and discussion

To buckling temperature analysis, the material properties of the CNT fiber and PMMA (poly (methyl

Table 1 Effective parameter of the CNT
(Shen and Xiang 2013, Mehar *et al.* 2019)

V_{NT}^*	η_1	η_2	η_3
0.12	0.137	1.022	0.715
0.17	0.142	1.626	1.138
0.28	0.141	1.585	1.109

methacrylate) matrix are assumed as temperature dependent and taken as same as in (Shen and Zhu 2010): $\rho = 1150$ kg/m^3, $E_m = (35.2 - 0.034T) \times 10^8$ Pa and $\alpha_m = 4.5(1 + 0.0005 \Delta T) \times 10^{-5}$, where, $\Delta T = T - T_0$ and $T_0 = 300$ K. The material properties of the CNT are provided in Eq. (24) and effectiveness parameters are explai1ned in Table 1 (Mirzaei and Kiani 2016).

$$\left.\begin{array}{l} E_{1NT}(\text{Pa}) = 6.3998\times10^{12} - 4.338417\times10^9T + 7.43\times10^6T^2 - 4.45833\times10^3T^3 \\ E_{2NT}(\text{Pa}) = 8.02155\times10^{12} - 5.420375\times10^9T + 9.275\times10^6T^2 - 5.5625\times10^3T^3 \\ G_{12NT}(\text{Pa}) = 1.40755\times10^{12} + 3.476208\times10^9T - 6.965\times10^6T^2 + 4.479167\times10^3T^3 \\ \alpha_{1NT}(10^{-6}/K) = -1.12515 + 22.9169\times10^{-3}T - 28.87\times10^{-6}T^2 + 113625\times10^{-9}T^3 \\ \alpha_{2NT}(10^{-6}/K) = 5437.15\times10^{-3} - 98.4625\times10^{-6}T + 29\times10^{-8}T^2 + 12.5\times10^{-12}T^3 \end{array}\right\} (24)$$

A personalized computer code has been established using MATLAB computer language to observe the critical buckling temperature and solved via FEM. The accuracy and reliability of the developed numerical model are checked by convergence and comparison studies.

3.1 Convergence and comparison study

FEA gives approximate result and the approximation can be improved by increase the number of the element. Conversely, the cost of computational will grow up when mesh size rises. In order to maintain the the accuaracy with minimum computational cost, the convergence study is an essential process.

Fig. 2 shows the convergence rate of the FG-CNTRC structure for two type thermal field (UDT and LDT) and four type shell geometries (CYL, SPH, HYP and ELL) with variable mesh size. In which other design parameters are fixed FG-X, $R/a = 5$, $a/h = 50$, $a/b = 1$ and $V_{NT}^* = 0.17$. The convergence analysis, indicate that the 6×6 mesh size is the optimal mesh size to maintain the balance between accuracy and computational cost for thermal buckling analysis.

Further, in order to assure the efficacy of newly developed graded finite element model, the critical buckling temperature of the FG-CNTRC plate is computed for three grading patterns and compared with the previously published result of Mirzaei and Kiani (2016). Fig. 3 depicted the comparison of of the buckling temperature for three CNT volume fraction and three grading configura-
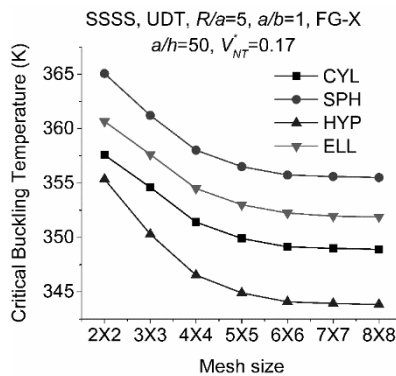
(a) UDT
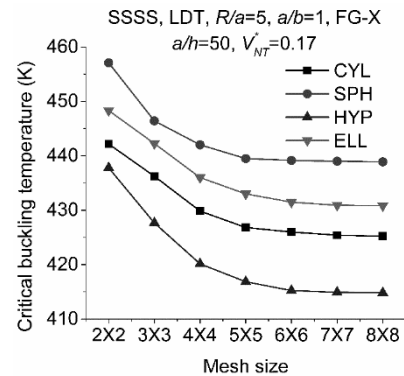
(b) LDT

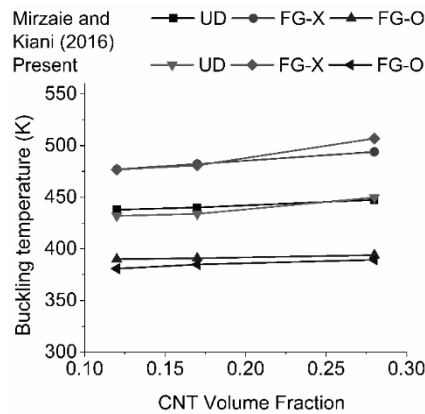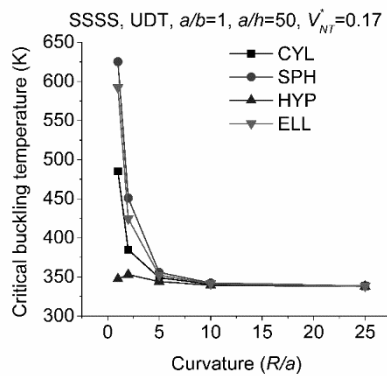Fig. 2 Convergence of the buckling temperature of CNTRC

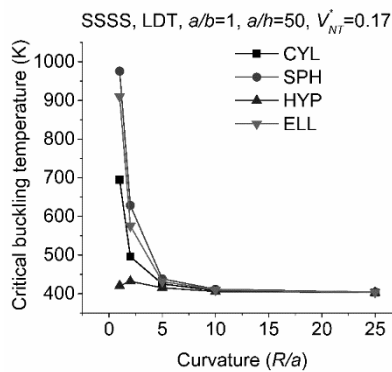Fig. 3 Comparison of buckling temperature of FG-CNTRC plate

tions. The figure depicted that the numerical results obtained using the present developed HSDT kinematic model and results of literature conforming with each other for all grading configurations.

3.2 Numerical analysis

After examine the required convergence and the comparison of the critical buckling parameters under the variable temperature loading, the analysis further extends to

show the effect of different design related input values on the buckling temperature. The critical thermal buckling responses computed using the current multiscale higher-order model for the said input variables and depicted in Figs. 4-7.

In curved shell structure, the curvature ratio depicts a major role on the stiffness of shell structure. To declare the same, the thermal stability of uniformly distributed CNTRC structure has been analyzed for five vales of curvature ratio (R/a = 1, 2, 5, 10 and 25) and four different shell panel (SPH, ELL, CYL and HYP) under two different thermal field (UDT and LDT) and other design parameters taken as a/h = 50, a/b = 1, V_{NT}^* = 0.17. Fig. 4 depicted that the critical buckling temperature of the CNTRC structure decreases when the curvature ratio increases. Also, the results indicate that the critical temperature values are higher for the LDT while compared to the UDT.

Fig. 5 illustrated the consequence of length to thickness ratio on the thermal stability of the graded CNTRC cylindrical panel under the various thermal fields (UDT and LDT), R/a = 50, a/b = 1 and V_{NT}^* = 0.17. It is understood that the cylindrical shell panel losses the stiffness with higher thickness ratio consequently the thermal performance of the composite structure degraded. The clamped shell buckling temperature values are higher for the of the clamped shell panel while compared to the simply supported shell panel.

The buckling behavior analysis extended for the different CNT volume fraction (V_{NT}^* = 0.12, 0.17 and 0.28) and presented in Fig. 6 and it is visualized that the thermal stability of the curved shell panel increases with higher

(a) UDT

(b) LDT

Fig. 4 Critical buckling temperature of CNTRC structure for variable curvature ratio
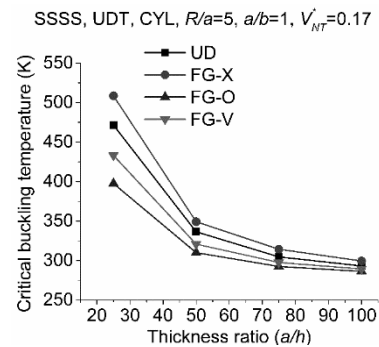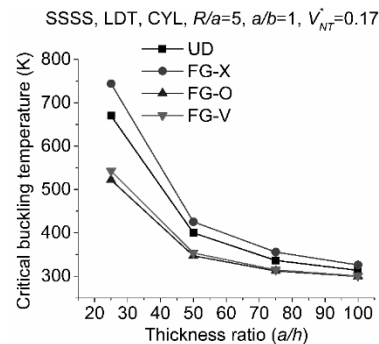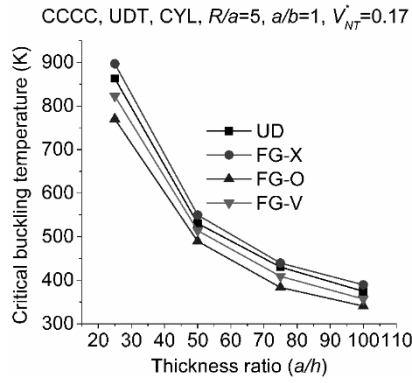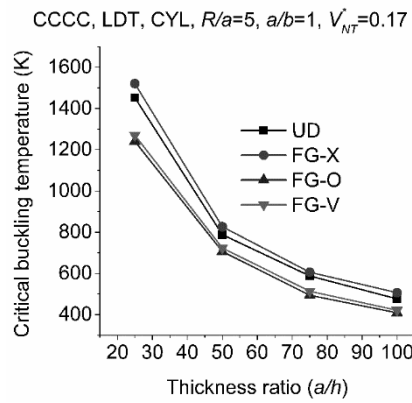

(a) UDT, SSSS

(b) LDT, SSSS

Fig. 5 Critical buckling temperature of CNTRC structure for various length to thickness ratio

(c) UDT, CCCC

(d) LDT, CCCC

Fig. 5 Continued

CNT volume fraction irrespective of the shell geometries and the spherical shell geometries show the highest thermal stability. To examine the same, the geometrical properties are taken as $R/a = 50$, $a/b = 1$ and $a/h = 50$ with simply supported condition.

Further, the buckling behavior of the shell panel is evaluated by varying the aspect ratio and presented in Table 2 for five aspect ratios ($a/b = 0.8$, 1.1, 1.4, 1.7 and 2) and four grading configurations (UD, FG-X, FG-O and FG-V). The critical buckling temperature is calculated for a cylindrical shell panel with all edges clamped condition, $R/a = 5$ and $a/h = 50$. It can be understood from the table

Table 2 Effect of aspect ratio on thermal instability of CNT reinforced cylindrical shell panel

Aspect ratio (a/b)	Grading patterns			
	UD	FG-X	FG-O	FG-V
0.8	520.065	537.616	487.346	507.676
1.1	530.773	549.017	493.525	517.006
1.4	541.869	562.245	493.183	523.272
1.7	546.064	564.956	506.317	533.352
2	570.397	589.329	508.311	562.020

that the higher temperature is required to buckle the graded CNTRC shell when aspect ratio is high. Because the width (b) of the shell panel decreases with higher aspect ratio (a/b) and shell panel are under clamped condition.

4. Conclusions

The critical buckling temperature of the FG-CNTRC shell panel is computed numerically using the currently proposed and derived HSDT displacement model. The governing equilibrium equation is obtained using the variational principle and solved through an own homemade code (MATLAB platform). Firstly, the convergence and comparison study has been conducted to build the necessary confidence and extended for the parametric analysis. Subsequent understanding related to the parametric analysis are discussed in point-wise form in the following lines.

(1) The critical buckling temperature of the FG-CNTRC shell panel increases with higher CNT volume fraction (V_{NT}^*) and aspect ratio (a/b) of the composite shell panel.
(2) The critical buckling temperature of the CNTRC shell panel is decreases with higher thickness ratio (a/h) and curvature ratio (R/a).
(3) Spherical shell panel is the stiffest geometry and the critical buckling temperature of the spherical shell panel is maximum as compared to other used geometries.
(4) The study indicates that to buckle the nanocom-
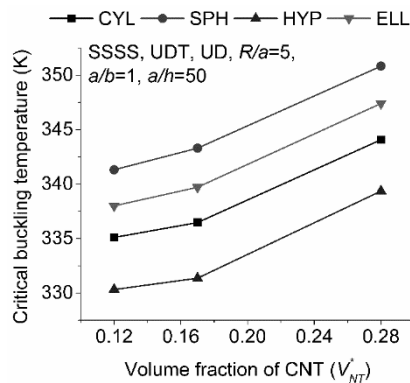
(a) UDT
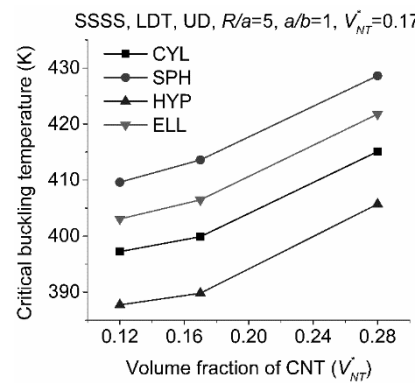
(b) LDT

Fig. 6 Effect of CNT volume fraction on critical buckling temperature of CNTRC

posite structure, a higher value of temperature required when panel is under the LDT in comparison to UDT.

(5) The critical buckling temperature for the FG-X type graded composite is maximum and minimum for FG-O.

References

Amabili, M. and Tajahmadi, M.R.S. (2012), "Thermal post-buckling of laminated and isotropic rectangular plates with fixed edges: Comparison of experimental and numerical results", *Proc. Inst. Mech. Eng. Part C J. Mech. Eng. Sci.*, **226**, 2393-2401. DOI: 10.1177/0954406211434496

Ansari, R. and Torabi, J. (2016), "Numerical study on the buckling and vibration of functionally graded carbon nanotube-reinforced composite conical shells under axial loading", *Compos. Part B Eng.*, **95**, 196-208. DOI: 10.1016/j.compositesb.2016.03.080

Ansari, R., Torabi, J. and Shojaei, M.F. (2017), "Buckling and vibration analysis of embedded functionally graded carbon nanotube-reinforced composite annular sector plates under thermal loading", *Compos. Part B Eng.*, **109**, 197-213. DOI: 10.1016/j.compositesb.2016.10.050

Arani, A.G. and Kolahchi, R. (2016), "Buckling analysis of embedded concrete columns armed with carbon nanotubes", *Comput.   Concr.*,   **17**,   567-578.   DOI: 10.12989/cac.2016.17.5.567

Arani, A.G., Kolahchi, R. and Vossough, H. (2012), "Buckling analysis and smart control of SLGS using elastically coupled PVDF nanoplate based on the nonlocal Mindlin plate theory", *Phys. B Condens Matter*, **407**, 4458-4465. DOI: 10.1016/j.physb.2012.07.046

Arani, A.G., Abdollahian, M., Kolahchi, R. and Rahmati, A.H. (2013), "Electro-thermo-torsional buckling of an embedded armchair DWBNNT using nonlocal shear deformable shell mode", *Compos. Part B Eng.*, **51**, 291-299. DOI: 10.1016/J.COMPOSITESB.2013.03.017

Arani, A.G., Jafari, G.S. and Kolahchi, R. (2017), "Nonlinear vibration analysis of viscoelastic micro nano-composite sandwich plates integrated with sensor and actuator", *Microsyst. Technol.*, **23**, 1509-1535. DOI: 10.1007/s00542-016-3095-9

Baiz, P.M. and Aliabadi, M.H. (2007), "Buckling analysis of shear deformable shallow shells by the boundary element method", *Eng. Anal. Bound Elem.*, **31**, 361-372. DOI: 10.1016/j.enganabound.2006.07.008.

Bakora, A. and Tounsi, A. (2015), "Thermo-mechanical post-buckling behavior of thick functionally graded plates resting on elastic foundations", *Struct. Eng. Mech., Int. J.*, **56**(1), 85-106. DOI: 10.12989/sem.2015.56.1.085

Barzoki, A.A.M., Arani, A.G., Kolahchi, R. and Mozdianfard, M.R. (2012), "Electro-thermo-mechanical torsional buckling of a piezoelectric polymeric cylindrical shell reinforced by DWBNNTs with an elastic core", *Appl. Math. Model.*, **36**, 2983-2995. DOI: 10.1016/J.APM.2011.09.093

Baseri, V., Jafari, G.S. and Kolahchi, R. (2016), "Analytical solution for buckling of embedded laminated plates based on higher order shear deformation plate theory", *Steel Compos. Struct., Int. J.*, **21**, 883-919. DOI: 10.12989/scs.2016.21.4.883

Berrabah, H.M., Tounsi, A., Semmah, A. and Bedia, E.A.A. (2013), "Comparison of various refined nonlocal beam theories for bending, vibration and buckling analysis of nanobeams", *Struct. Eng. Mech., Int. J.*, **48**(3), 351-365. DOI: 10.12989/sem.2013.48.3.351

Bouadi, A., Bousahla, A.A., Houari, M.S.A., Heireche, H. and Tounsi, A. (2018), "A new nonlocal HSDT for analysis of

stability of single layer graphene sheet", *Adv. Nano Res., Int. J.*, **6**(2), 147-162. DOI: 10.12989/anr.2018.6.2.147

Bouguenina, O., Belakhdar, K., Tounsi, A. and Bedia, E.A.A. (2015), "Numerical analysis of FGM plates with variable thickness subjected to thermal buckling", *Steel Compos. Struct., Int. J.*, **19**(3), 679-695. DOI: 10.12989/scs.2015.19.3.679

Bouhadra, A., Benyoucef, S. and Tounsi, A. (2015), "Thermal buckling response of functionally graded plates with clamped boundary conditions", *J. Therm. Stress*, **38**, 630-650. DOI: 10.1080/01495739.2015.1015900

Brighenti, R. (2005a), "Numerical buckling analysis of compressed or tensioned cracked thin plates", *Eng. Struct.*, **27**, 265-276. DOI: 10.1016/j.engstruct.2004.10.006

Brighenti, R. (2005b), "Buckling of cracked thin-plates under tension or compression", *Thin-Wall. Struct.*, **43**, 209-224. DOI: 10.1016/j.tws.2004.07.006

Cook, R.D., Malkus, D.S., Plesha, M.E. and Witt, R.J. (2009), *Concepts and Applications of Finite Element Analysis*, *Fourth edi*, John Wiley & Sons Pvt. Ltd., Singapore.

Draiche, K., Tounsi, A. and Khalfi, Y. (2014), "A trigonometric four variable plate theory for free vibration of rectangular composite plates with patch mass", *Steel Compos. Struct., Int. J.*, **17**(1), 69-81. DOI: 10.12989/scs.2014.17.1.069

Duc, N.D., Cong, P.H. and Tuan, N.D. (2017), "Thermal and mechanical stability of functionally graded carbon nanotubes (FG CNT)-reinforced composite truncated conical shells surrounded by the elastic foundations", *Thin-Wall. Struct.*, **115**, 300-310. DOI: 10.1016/j.tws.2017.02.016

Fantuzzi, N., Tornabene, F., Bacciocchi, M. and Dimitri, R. (2017), "Free vibration analysis of arbitrarily shaped functionally graded carbon nanotube-reinforced plates", *Compos. Part B Eng.*, **115**, 384-408. DOI: 10.1016/j.compositesb.2016.09.021

Farzam, A. and Hassani, B. (2018), "Thermal and mechanical buckling analysis of FG carbon nanotube reinforced composite plates using modified couple stress theory and isogeometric approach", *Compos. Struct.*, **206**, 774-790.

Fazzolari, F.A. (2015), "Natural frequencies and critical temperatures of functionally graded sandwich plates subjected to uniform and non-uniform temperature distributions", *Compos. Struct.*, **121**, 197-210. DOI: 10.1016/j.compstruct.2014.10.039

Hajmohammad, M.H., Zarei, M.S., Nouri, A. and Kolahchi, R. (2017), "Dynamic buckling of sensor/functionally graded-carbon nanotube-reinforced laminated plates/actuator based on sinusoidal-visco-piezoelasticity theories", *J. Sandw. Struct. Mater.*, 109963621772037. DOI: 10.1177/1099636217720373

Hamidi, A., Houari, M.S.A., Mahmoud, S.R.R. and Tounsi, A. (2015), "A sinusoidal plate theory with 5-unknowns and stretching effect for thermomechanical bending of functionally graded sandwich plates", *Steel Compos. Struct., Int. J.*, **18**(1), 235-253. DOI: 10.12989/scs.2015.18.1.235

Han, Q., Wang, Z., Nash, D.H. and Liu, P. (2017), "Thermal buckling analysis of cylindrical shell with functionally graded material coating", *Compos. Struct.*, **181**, 171-182.

Kiani, Y. (2017), "Buckling of FG-CNT-reinforced composite plates subjected to parabolic loading", *Acta Mech.*, **228**, 1303-1319. DOI: 10.1007/s00707-016-1781-4

Kiani, Y., Dimitri, R. and Tornabene, F. (2018), "Free vibration study of composite conical panels reinforced with FG-CNTs", *Eng. Struct.*, **172**, 472-482. DOI: 10.1016/j.engstruct.2018.06.006

Kolahchi, R. (2017), "A comparative study on the bending, vibration and buckling of viscoelastic sandwich nano-plates based on different nonlocal theories using DC, HDQ and DQ methods", *Aerosp. Sci. Technol.*, **66**, 235-248. DOI: 10.1016/j.ast.2017.03.016

Kolahchi, R. and Cheraghbak, A. (2017), "Agglomeration effects on the dynamic buckling of viscoelastic microplates reinforced with SWCNTs using Bolotin method", *Nonlinear Dyn.*, **90**, 479-492. DOI: 10.1007/s11071-017-3676-x

Kolahchi, R., Bidgoli, M.R., Beygipoor, G. and Fakhar, M.H. (2015), "A nonlocal nonlinear analysis for buckling in embedded FG-SWCNT-reinforced microplates subjected to magnetic field", *J. Mech. Sci. Technol.*, **29**, 3669-3677. DOI: 10.1007/s12206-015-0811-9

Kolahchi, R., Zarei, M.S., Hajmohammad, M.H., Oskouei, A.N. (2017), "Visco-nonlocal-refined Zigzag theories for dynamic buckling of laminated nanoplates using differential cubature-Bolotin methods", *Thin-Wall. Struct.*, **113**, 162-169. DOI: 10.1016/j.tws.2017.01.016

Lei, Z.X., Zhang, L.W. and Liew, K.M. (2015), "Buckling of FG-CNT reinforced composite thick skew plates resting on Pasternak foundations based on an element-free approach", *Appl. Math. Comput.*, **266**, 773-791. DOI: 10.1016/j.amc.2015.06.002

Maghamikia, S. and Jam, J.E. (2011), "Buckling analysis of circular and annular composite plates reinforced with carbon nanotubes using FEM", *J. Mech. Sci. Technol.*, **25**, 2805-2810. DOI: 10.1007/s12206-011-0738-8

Mahapatra, T.R., Mehar, K., Panda, S.K., Dewangan, S. and Dash, S. (2017), "flexural strength of functionally graded nanotube reinforced sandwich spherical panel", *Proceeding of IOP Conference Series*: *Materials Science and Engineering*, **178**, 012031.

Mayandi, K. and Jeyaraj, P. (2015), "Bending, buckling and free vibration characteristics of FG-CNT polymer composite beam under non-uniform thermal load", *J. Mater. Des. Appl.*, **229**, 13-28. DOI: 10.1177/1464420713493720

Mehar, K. and Panda, S.K. (2018a), "Elastic bending and stress analysis of carbon nanotube-reinforced composite plate: Experimental, numerical, and simulation", *Adv. Polym. Technol.*, **37**, 1643-1657. DOI: 10.1002/adv.21821

Mehar, K. and Panda, S.K. (2018b), "Nonlinear finite element solutions of thermoelastic flexural strength and stress values of temperature dependent graded CNT-reinforced sandwich shallow shell structure", *Struct. Eng. Mech.*, *Int. J.*, **67**(6), 565-578. DOI: 10.12989/sem.2018.67.6.565

Mehar, K. and Panda, S.K. (2018c), "Thermal free vibration behavior of FG-CNT reinforced sandwich curved panel using finite element method", *Polym. Compos.*, **39**, 2751-2764. DOI: 10.1002/pc.24266

Mehar, K. and Panda, S.K. (2018d), "Thermoelastic flexural analysis of FG-CNT doubly curved shell panel", *Aircr. Eng. Aerosp. Technol.*, **90**, 11-23. DOI: 10.1108/AEAT-11-2015- 0237.R2

Mehar, K., Panda, S.K., Devarajan, Y. and Choubey, G. (2019), "Numerical buckling analysis of graded CNT-reinforced composite sandwich shell structure under thermal loading", *Compos. Struct.* DOI: https://doi.org/10.1016/j.compstruct.2019.03.002

Mehrabadi, S.J., Aragh, B.S., Khoshkhahesh, V. and Taherpour, A. (2012), "Mechanical buckling of nanocomposite rectangular plate reinforced by aligned and straight single-walled carbon nanotubes", *Compos*, *Part B Eng.*, **43**, 2031-2040. DOI: 10.1016/j.compositesb.2012.01.067

Mirzaei, M. and Kiani, Y. (2016), "Thermal buckling of temperature dependent FG-CNT reinforced composite plates", *Meccanica*, **51**, 2185-2201. DOI: 10.1007/s11012-015-0348-0

Moradi-Dastjerdi, R., Pourasghar, A., Foroutan, M. and Bidram, M. (2014), "Vibration analysis of functionally graded nanocomposite cylinders reinforced by wavy carbon nanotube based on mesh-free method", *J. Compos. Mater.*, **48**, 1901-1913. DOI: 10.1177/0021998313491617

Moradi-dastjerdi, R., Malek-mohammadi, H. and Mohammadi, H.M. (2017), "Free vibration and buckling analyses of functionally graded nanocomposite plates reinforced by carbon nanotube", *Mech. Adv. Compos. Struct.*, **4**, 59-73. DOI: 10.22075/MACS.2016.496

Nejati, M., Dimitri, R., Tornabene, F. and Hossein Yas, M. (2017), "Thermal buckling of nanocomposite stiffened cylindrical shells reinforced by functionally graded wavy carbon nanotubes with temperature-dependent properties", *Appl. Sci.*, **7**(12), 1223.

Pandya, B.N. and Kant, T. (1988), "Finite element analysis of laminated composite plates using a higher-order displacement model", *Compos. Sci. Technol.*, **32**, 137-155. DOI: 10.1016/0266-3538(88)90003-6

Rafiee, M., Yang, J. and Kitipornchai, S. (2013), "Thermal bifurcation buckling of piezoelectric carbon nanotube reinforced composite beams", *Comput. Math. Appl.*, **66**(7), 1147-1160.

Rafiee, M., Nitzsche, F. and Labrosse, M.R. (2018), "Modeling and mechanical analysis of multiscale fiber-reinforced graphene composites: Nonlinear bending, thermal post-buckling and large amplitude vibration", *Int. J. Non-Linear Mech.*, **103**, 104-112.

Reddy, B.S., Kumar, J.S., Reddy, C.E. and Reddy, K. (2013), "Buckling analysis of functionally graded material plates using higher order shear deformation theory", *J. Compos.*

Sharma, N., Mahapatra, T.R., Panda, S.K. and Mehar, K. (2018), "Evaluation of vibroacoustic responses of laminated composite sandwich structure using higher-order finite-boundary element model", *Steel Compos. Struct.*, *Int. J.*, **28**(5), 629-639. DOI: 10.12989/scs.2018.28.5.629

Shen, H.S. (2009), "Nonlinear bending of functionally graded carbon nanotube-reinforced composite plates in thermal environments", *Compos Struct*, **91**,9–19, doi: 10.1016/j.compstruct.2009.04.026.

Shen, H.S. (2011), "Postbuckling of nanotube-reinforced composite cylindrical shells in thermal environments, Part I: Axially-loaded shells", *Compos Struct*, **93**,2096–2108, doi: 10.1016/j.compstruct.2011.02.011.

Shen, H.S. (2012), "Thermal buckling and postbuckling behavior of functionally graded carbon nanotube-reinforced composite cylindrical shells", *Compos. Part B Eng.*, **43**, 1030-1038. DOI: 10.1016/j.compositesb.2011.10.004

Shen, H.S. and Xiang, Y. (2013), "Nonlinear analysis of nanotube-reinforced composite beams resting on elastic foundations in thermal environments", *Eng. Struct.*, **56**, 698-708. DOI: 10.1016/j.engstruct.2013.06.002

Shen, H.S. and Zhang, C.L. (2010), "Thermal buckling and postbuckling behavior of functionally graded carbon nanotube-reinforced composite plates", *Mater. Des.*, **31**, 3403-3411. DOI: 10.1016/j.matdes.2010.01.048

Shen, H.S. and Zhu, Z.H. (2010), "Buckling and postbuckling behavior of functionally graded nanotube-reinforced composite plates in thermal environments", *C. Comput. Mater. Contin.*, **18**, 155-182.

Swaminathan, K., Naveenkumar, D.T., Zenkour, A.M. and Carrera, E. (2015), "Stress, vibration and buckling analyses of FGM plates-A state-of-the-art review", *Compos. Struct.*, **120**, 10-31.

Szekrenyes, A. (2012), "Interlaminar stresses and energy release rates in delaminated orthotropic composite plates", *Int. J. Solids Struct.*, **49**, 2460-2470. DOI: 10.1016/j.ijsolstr.2012.05.010

Szekrenyes, A. (2014), "Analysis of classical and first-order shear deformable cracked orthotropic plates", *J. Compos. Mater.*, **48**, 1441-1457. DOI: 10.1177/0021998313487756

Togun, N. (2016), "Nonlinear vibration of nanobeam with attached mass at the free end via nonlocal elasticity theory", *Microsyst. Technol.*, **22**, 2361-2362. DOI: 10.1007/s00542-016-3082-1

Tohidi, H., Hosseini-Hashemi, S.H. and Maghsoudpour, A. (2017), "Nonlinear size-dependent dynamic buckling analysis of embedded micro cylindrical shells reinforced with agglomerated

CNTs using strain gradient theory", *Microsyst. Technol.*, **23**, 5727-5744. DOI: 10.1007/s00542-017-3407-8

Torabi, J., Ansari, R. and Hassani, R. (2019), "Numerical study on the thermal buckling analysis of CNT-reinforced composite plates with different shapes based on the higher-order shear deformation theory", *Eur. J. Mech.-A/Solids*, **73**, 144-160.

Tornabene, F., Bacciocchi, M., Fantuzzi, N. and Reddy, J.N. (2017), "Multiscale approach for three-phase CNT/polymer/ fiber laminated nanocomposite structures", *Polym. Compos.*, **16**, 101-113. DOI: 10.1002/pc.24520

Yang, J., Ke, L.L. and Feng, C. (2015), "Dynamic buckling of thermo-electro-mechanically loaded FG-CNTRC beams", *Int. J. Struct. Stab. Dyn.*, **15**, 1-17.
DOI: 10.1142/S0219455415400179

Zenkour, A.M. (2005), "A comprehensive analysis of functionally graded sandwich plates: Part 2-Buckling and free vibration", *Int J. Solids Struct.*, **42**, 5243-5258.
DOI: 10.1016/j.ijsolstr.2005.02.016

Zhang, L.W., Lei, Z.X. and Liew, K.M. (2015a), "An element-free IMLS-Ritz framework for buckling analysis of FG-CNT reinforced composite thick plates resting on Winkler foundations", *Eng. Anal. Bound Elem.*, **58**, 7-17.
DOI: 10.1016/j.enganabound.2015.03.004

Zhang, L.W., Lei, Z.X. and Liew, K.M. (2015b), "Buckling analysis of FG-CNT reinforced composite thick skew plates using an element-free approach", *Compos. Part B Eng.*, **75**, 36-46. DOI: 10.1016/j.compositesb.2015.01.033

Zidour, M., Daouadji, T.H., Benrahou, K.H., Tounsi, A., Bedia, E.A.A. and Hadji, L. (2014), "Buckling analysis of chiral single-walled carbon nanotubes by using the nonlocal Timoshenko beam theory", *Mech. Compos. Mater.*, **50**, 95-104.
DOI: 10.1007/s11029-014-9396-0

CC